

Interactive Dendritic Spine Analysis Based on 3D Morphological Features

JunYoung Choi*

Ulsan National Institute of Science and Technology

Eunji Cho‡

Seoul National University College of Medicine

Sunghoe Chang^{||}

Seoul National University College of Medicine

Sang-Eun Lee[†]

Seoul National University College of Medicine

Yutaro Kashiwagi[§]

Shigeo Okabe^{||}

University of Tokyo

University of Tokyo

Won-Ki Jeong**

Ulsan National Institute of Science and Technology

ABSTRACT

Dendritic spines are submicron scale protrusions on neuronal dendrites that form the postsynaptic sites of excitatory neuronal inputs. The morphological changes of dendritic spines reflect alterations in physiological conditions and are further indicators of various neuropsychiatric conditions. However, due to the highly dynamic and heterogeneous nature of spines, accurate measurement and object analysis of spine morphology is a major challenge in neuroscience research. Here, we propose an interactive 3D dendritic spine analysis system that displays 3D rendering of spines and plots the high-dimensional features extracted from the 3D mesh of spines in three graph types (parallel coordinate plot, radar plot, and 2D scatter plot with t-Distributed Stochastic Neighbor Embedding). With this system, analysts can effectively explore and analyze the dendritic spine in a 3D manner with high-dimensional features. For the system, we have constructed a set of morphological high-dimensional features from the 3D mesh of dendritic spines.

Index Terms: Biomedical and Medical Visualization ; Coordinated and Multiple Views ; User Interfaces

1 INTRODUCTION

Dendritic spines are small, specialized protrusions from neuronal dendrites that are postsynaptic structures in the majority of excitatory synapses (Figure 1). Typically, dendritic spines have a round-shaped head (Figure 1e) and a narrow neck (Figure 1d) that connects the head to the dendritic shaft [10, 13]. A single neuron contains hundreds of spines of various sizes and shapes. Dendritic spines play a critical role in the formation of new neural circuits and synaptic plasticity, and also serve as a potential substrate for various neuropsychiatric disorders, especially those with deficits in information processing [11]. The morphology of dendritic spines is a critical determinant of the function of spines, and recent studies indicate that spines are highly motile and undergo morphologic changes over the extensive spatiotemporal range depending on neuronal development and synaptic activity. Thus, precise measurement and object analysis of spine morphology is required to understand the physiological regulation of excitatory synaptic transmission and pathological changes in the process [1].

Existing spine analysis methods are mostly based on 2D microscopy images, and several earlier studies introduced computa-

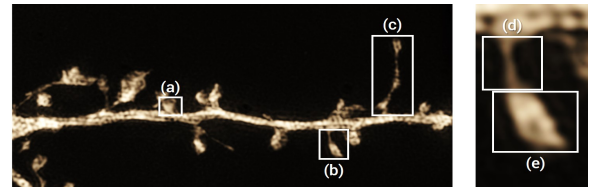


Figure 1: An example of dendritic spines. (a), (b), and (c) are spines of different types connected to the dendrite shaft. (d) is the neck and (e) is the head part of the spine (b).

tional methods to extract the structural features of the spine from the 2D microscopy images [9, 14, 20]. And, several recent papers have calculated the 3D morphological features of spines, and analyzed the spines accordingly [2, 8]. Those previous work aimed to construct quantitative measures using 2D or 3D morphological features to analyze spines. However, existing 2D approaches may underestimate the great heterogeneity in spine size and shape [5, 19] and could lead to a biased view of spine morphology [16]. Also, existing 3D approaches allow only limited analysis, such as grouping the spines into several known groups. More importantly, there exists no visualization tool that allows users to visually explore 3D geometry and high-dimensional morphological features of dendritic spines and to conduct on-line data analysis using various visualization.

To address these problems, we propose a novel interactive visual analysis system for dendritic spines using 3D geometry-based high-dimensional features. The system provides an interactive data exploration interface that allows users to easily compare and analyze multiple dendritic spines via 3D surface rendering and multi-dimensional feature plots (e.g., radar chart, parallel coordinate, and t-SNE plots). We also propose a new ten-dimensional morphological feature that extends previous work [8, 12], and demonstrate its effectiveness for subtle comparison analysis cases that can easily lead to wrong analysis by using conventional features.

2 BACKGROUND AND RELATED WORK

2.1 Dendritic Spine

An ideal and mature spine contains a bulbous head that is connected with the main dendrite by a narrow neck. The most widely used nomenclature divides the dendritic spines into three phenotypes based on the relative sizes of the spine head and neck [24]; mushroom spines with a large head and a narrow neck (Figure 1b); thin spines with a smaller head and a narrow neck (Figure 1c); and stubby spines without an obvious constriction between the head and the neck (Figure 1a). Filopodia, which has the hair-like shape, can also be classified into another phenotype.

Tackenberg *et al.* [23] introduced that the phenotype of spine is closely related to the strength of synaptic transmission and is associated with neurological disorders such as Alzheimer's disease. So, the accurate phenotype classification is essential in this research area. Furthermore, if we can precisely track changes in the phenotype distribution of the spines in specific neural area, we can predict

*e-mail: juny0603@unist.ac.kr

†e-mail: sangeun45@snu.ac.kr

‡e-mail: eunji0623@snu.ac.kr

§e-mail: kashiwagi@u-tokyo.ac.jp

||e-mail: okabe@u-tokyo.ac.jp

||e-mail: sunghoe@snu.ac.kr

**e-mail: wkjeong@unist.ac.kr

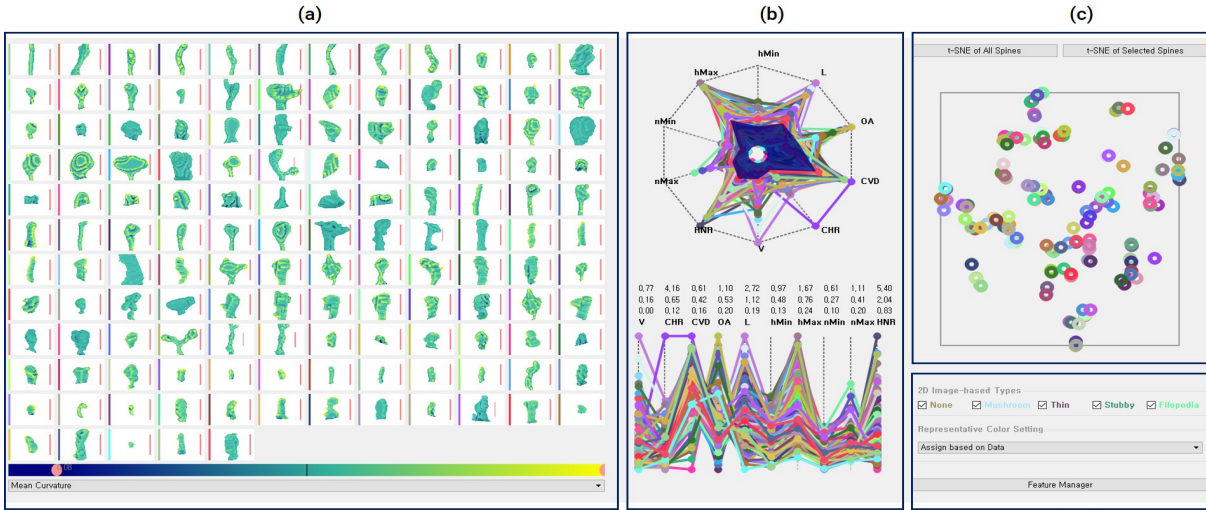


Figure 2: An overview of proposed system. (a): This shows the rendering of the spines to be displayed in grid layout. (b): A feature plot shows the 10D features represented as shapes (radar plot) and lines (parallel coordinate plot). (c): A feature similarity plot shows the possible clusters. (d): The controls include useful functions to enable effective analysis.

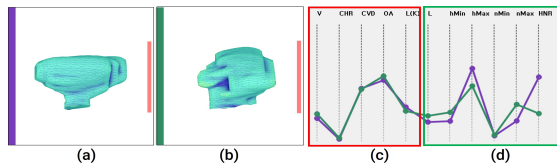


Figure 3: The five-dimensional features (c) used in [8] cannot distinguish (a) and (b). However, these spines can be distinguished with our new 3D morphological feature set (d).

the putative trajectory of dendritic spine pathology and furthermore obtain the prognosis of patients with the disease.

2.2 Analysis of Dendritic Spines

Several studies have reported computational methods for modeling dynamic spine behaviors and for object structural classification of spines. The 2D tracing algorithm using a curvilinear structure detector for dendrite analysis [25] and an automated spine analysis algorithm were reported [18]. However, 2D analysis failed to include information of dendritic spines extending to the z-plane. Another study used a commercially available Imaris software to analyze dendritic spines using three simple structural parameters [22]. NeuronStudio based on the Rayburst sampling algorithm was also used for analyzing spine structure but the three key parameters (aspect ratio, head-to-neck ratio, and spine head diameter) are not suitable for the complex nature of the 3D spine structure [15].

For sophisticated and accurate analysis, several recent papers have calculated the 3D morphological features of spines, and classified the spines accordingly [2, 8]. Kashiwagi *et al.* [8] introduced a 5-dimensional 3D morphological feature; Volume (V); convex hull ratio (CHR); coefficient of variation in distance (CVD); open angle (OA); and estimated spine length (EL). These features were used to classify spines into mushroom and nonmushroom types through Principal Component Analysis (PCA) [7] and support vector machine (SVM) [21]. While the above 5-dimensional features can effectively represent complex and diverse 3D shapes, they cannot distinguish some of spines which are included in the different types because they do not reflect a spine’s unique characteristics such as the neck and head. For example, Figure 3a is close to the mushroom type, and Figure 3b is close to the stubby type. However, there is no difference in the five features (Figure 3c) between the two spines in this case.

2.3 High-Dimensional Morphological Features

Data for computational geometry of dendritic spines in primary cultured hippocampal neurons were prepared as described previously in Kashiwagi *et al.* [8]. In this work, a structured illumination microscopy (SIM) is used to extract accurate shape of neuron. By comparing this method with an electron microscopic (EM)-based method, they verified that this method enables accurate 3D morphological measurement. Based on this observation, we designed and evaluated the proposed system with the premise that the reconstructed 3D spine mesh is faithfully representing the shape of spine.

To address the limitations of Kashiwagi *et al.*’s 5-dimensional features, we propose a new 10-dimensional feature set by adding five 3D morphological features reflecting the intrinsic morphological properties of the spine’s head and neck (Figure 4). The 10-dimensional feature set includes V, CHR, CVD, OA, authentic spine length (L), maximum head diameter (hMax), minimum head diameter (hMin), maximum neck diameter (nMax), and minimum neck diameter (nMin). The hMax, hMin, nMax, nMin, and HNR are the 3D extensions of the 2D image-based features, maximum neck diameter, and maximum neck diameter, introduced by Qiao *et al.* [12]. We determine the maximum diameter as hMax and the minimum diameter as hMin in the local plane with the largest maximum diameter of the head part. Similarly, nMax and nMin are the maximum diameter and minimum diameter in the local plane with the smallest maximum diameter of the neck part. HNR is the ratio of head to neck, which is obtained by $\frac{hMax}{nMax}$.

Among the above 10-dimensional features, hMax, hMin, nMax, nMin, and HNR features represent the nature of spine such as neck and head, and V, CHR, CVD, OA, and L can represent the morphology of 3D mesh. So, this 10-dimensional feature set can reflect not only the nature of the spine, but also 3D morphology.

3 INTERACTIVE DENDRITIC SPINE ANALYSIS SYSTEM

The main goal of this system is to provide a method to compare and analyze multiple dendritic spines easily in a 3D-based manner. To achieve this goal, the system should arrange and visualize a large number of spines in a single view while allowing interactive 3D rendering of each spine. This system should also provide a way to compare high-dimensional features, find correlation between features and conduct analysis tasks. The following sections introduce the overall structure of the system (Section 3.1) and explain how the users can compare and analyze spines effectively (Section 3.2).

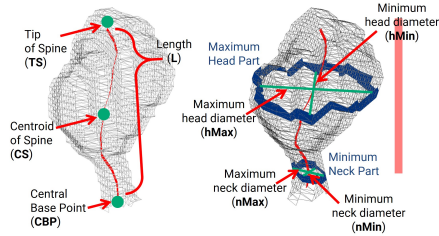


Figure 4: Five 3D morphological features (L, hMax, hMin, nMax, and nMin) representing the intrinsic properties of the spine (such as the size of neck and head).

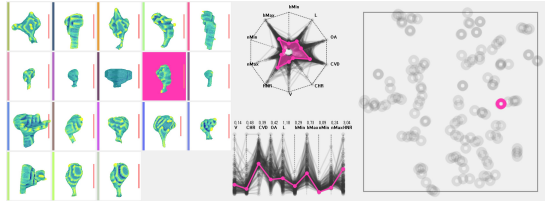


Figure 5: An example of the focusing function is shown. The background of the focused spine is colored pink. Only related lines and points are enabled.

3.1 System Design

The system's interface is divided into several groups (panels) based on their functions, such as a rendering panel, a high-dimensional feature plot panel, and a feature similarity plot panel. There is also a feature manager that can generate new features based on correlation between existing features. This interface layout was designed based on the interviews with the actual users of this system. The main design decision-making process behind each part is detailed below.

• Rendering panel

3D rendering: Observing the spine on a 2D image or at a fixed viewpoint can lead to a significant error in the analysis. The system can prevent this problem by rendering the spine in 3D and enabling rotation and zooming through the mouse interaction (Figure 6). Analysts can also see the actual size of the spine by placing a $1\mu\text{m}$ scale bar on the right side of each spine.

Functional color bar: Each spine has a color bar on the left side of the rendered spine with a **representative color**. Each spine has its own unique representative color that is randomly assigned. The color is also applied to the line of feature plot (Figure 2b) and point of feature similarity plot (Figure 2c). Thus, analysts can easily connect each spine to its own feature. When the user mouse is over the color bar, the background of the spine is changed to the color of the color bar, and only the feature line and point of that spine are enabled (**Focusing**: Figure 5b). In addition, clicking on the color bar will switch to a detailed view that shows only one spine on the entire rendering panel allowing users to closely observe the spine (Figure 6).

Spines placement with grid layout: Even with 3D-based observations, it is difficult to determine the phenotype of a single spine because spines have a highly dynamic and heterogeneous nature. In this system, multiple spines can be placed in one scene and compared and analyzed for effectively analyzing the phenotype. Some of the functions of the system, such as range selection and turn on/off the group or type allow users to select specific spines and the selected spines are placed on the $N \times N$ grid layout ($N = \lceil \sqrt{\text{Number of selected spines}} \rceil$) (Figure 2a).

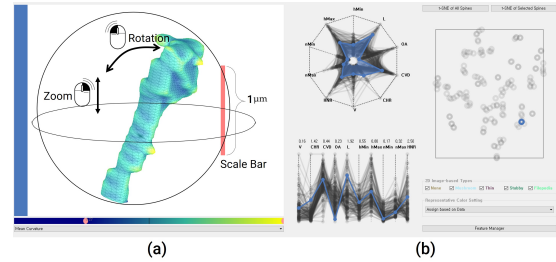


Figure 6: An example of the detailed view is shown. (a): A specific dendritic spine was rendered. Analysts can rotate the spine by dragging the mouse left and zoom in and out by dragging the mouse up and down. The red bar on the right side of the spine represents a micrometer. The color bar on the left side is a functional bar. (b): The line in the feature plots and the points in the similarity plots are colored by functional bar's color.

• High-dimensional feature plot panel

A radar plot and a parallel coordinate plot (Figure 2b) were used to compare and utilize the 10-dimensional feature extracted from the spines. The radar plot allows intuitive comparison between spines by showing high-dimensional features as a shape [17]. The blue area on the radar plot is the shape created by connecting the mean values of the features of the enabled spines. This shape allows intuitive comparison between different groups. A parallel coordinate plot represents high-dimensional features in parallel lines that features can be easily identified and utilized [6]. Above each axis of this plot, the minimum, average, and maximum values of the selected spines are displayed to show statistical values.

Interaction with feature plot panel: When the user's mouse hovers over a line of plot, the related spine focused and when the user clicks the line, the rendering panel is switched to a detailed view of the focused spine. User can select spines in a specific range by brushing on the each axis of plots. (Figure 7b: **Range Selection**)

• Feature similarity plot panel

We use t-Distributed Stochastic Neighbor Embedding (t-SNE) method to reduce the 10-dimensional data into 2-dimensions, so that it can easily group spines with similar features (Figure 2c). For effective analysis, user can perform t-SNE in real-time using only enabled spines or all spines.

Interaction with similarity plot panel: Similar to a feature plot panel, a mouse hovering over a specific point focuses on the spine, and when clicked it switches to the detailed view of the spine. In addition, a specific region can be selected by dragging the mouse, and then only the spines contained in the region will be enabled (Figure 7c: **Area Selection**). Similarity plot panel is based on similarity between the features of spines. Thus, in the panel, there are many unit clusters of spines with similar features, and the user can select similar spines by selecting specific cluster. On the right side of Figure 7c, one cluster is selected by area selection, and the selected spine shape, on the right side, is morphologically similar.

• Feature manager

In this system, we used ten features in total, four of them were introduced by Kashiwagi *et al.* [8] and six from the proposed morphological features. And, the user can generate additional useful features such as the ratio of L to hMax (LHR) by creating a formula in the feature manager. For example, the LHR can be added to the system by writing the expression $LHR = L / hMax$ in the text editor of the feature manager and pressing the Add Feature button. With this function, users can easily create new features for exploring correlation between features.

REFERENCES

- [1] J. I. Arellano, R. Benavides-Piccione, J. DeFelipe, and R. Yuste. Ultrastructure of dendritic spines: correlation between synaptic and spine morphologies. *Frontiers in neuroscience*, 1:10, 2007.
- [2] S. Basu, P. K. Saha, M. Roszkowska, M. Magnowska, E. Baczynska, N. Das, D. Plewczynski, and J. Wlodarczyk. Quantitative 3-d morphometric analysis of individual dendritic spines. *Scientific reports*, 8(1):3545, 2018.
- [3] E. Bertling, A. Ludwig, M. Koskinen, and P. Hotulainen. Methods for three-dimensional analysis of dendritic spine dynamics. *Methods in enzymology*, 506:391–406, 12 2012. doi: 10.1016/B978-0-12-391856-7.00043-3
- [4] D. L. Dickstein, A. Rodriguez, A. B. Rocher, S. L. Wearne, J. I. Luebke, C. M. Weaver, and P. R. Hof. Neuronstudio: An automated quantitative software to assess changes in spine pathology in alzheimer models. *Alzheimer's & Dementia: The Journal of the Alzheimer's Association*, 6(4):S410, 2010.
- [5] J. C. Fiala, M. Feinberg, V. Popov, and K. M. Harris. Synaptogenesis via dendritic filopodia in developing hippocampal area ca1. *Journal of Neuroscience*, 18(21):8900–8911, 1998.
- [6] A. Inselberg. *Parallel Coordinates: Interactive Visualisation for High Dimensions*, pp. 49–78. Springer London, London, 2009. doi: 10.1007/978-1-84800-269-2_3
- [7] I. Jolliffe. *Principal Component Analysis*, pp. 1094–1096. Springer Berlin Heidelberg, Berlin, Heidelberg, 2011. doi: 10.1007/978-3-642-04898-2_455
- [8] Y. Kashiwagi, T. Higashi, K. Obashi, Y. Sato, N. H. Komiyama, S. G. Grant, and S. Okabe. Computational geometry analysis of dendritic spines by structured illumination microscopy. *Nature Communications*, 10(1):1285, 2019.
- [9] P. Maiti, J. Manna, G. Ilavazhagan, J. Rossignol, and G. L. Dunbar. Molecular regulation of dendritic spine dynamics and their potential impact on synaptic plasticity and neurological diseases. *Neuroscience & Biobehavioral Reviews*, 59:208–237, 2015.
- [10] E. A. Nimchinsky, B. L. Sabatini, and K. Svoboda. Structure and function of dendritic spines. *Annual review of physiology*, 64(1):313–353, 2002.
- [11] P. Penzes, M. E. Cahill, K. A. Jones, J.-E. VanLeeuwen, and K. M. Woolfrey. Dendritic spine pathology in neuropsychiatric disorders. *Nature neuroscience*, 14(3):285, 2011.
- [12] H. Qiao, M.-X. Li, C. Xu, H.-B. Chen, S.-C. An, and X.-M. Ma. Dendritic spines in depression: what we learned from animal models. *Neural plasticity*, 2016, 2016.
- [13] A. Rao and A. M. Craig. Signaling between the actin cytoskeleton and the postsynaptic density of dendritic spines. *Hippocampus*, 10(5):527–541, 2000.
- [14] W. C. Risher, T. Ustunkaya, J. S. Alvarado, and C. Eroglu. Rapid golgi analysis method for efficient and unbiased classification of dendritic spines. *PloS one*, 9(9):e107591, 2014.
- [15] A. Rodriguez, D. B. Ehlenberger, D. L. Dickstein, P. R. Hof, and S. L. Wearne. Automated three-dimensional detection and shape classification of dendritic spines from fluorescence microscopy images. *PloS one*, 3(4):e1997, 2008.
- [16] B. Ruszczycycki, Z. Szepesi, G. M. Wilczynski, M. Bijata, K. Kalita, L. Kaczmarek, and J. Wlodarczyk. Sampling issues in quantitative analysis of dendritic spines morphology. *BMC bioinformatics*, 13(1):213, 2012.
- [17] M. J. Saary. Radar plots: a useful way for presenting multivariate health care data. *Journal of clinical epidemiology*, 61(4):311–317, 2008.
- [18] J. Son, S. Song, S. Lee, S. Chang, and M. Kim. Morphological change tracking of dendritic spines based on structural features. *Journal of microscopy*, 241(3):261–272, 2011.
- [19] J. Spacek and K. M. Harris. Three-dimensional organization of smooth endoplasmic reticulum in hippocampal ca1 dendrites and dendritic spines of the immature and mature rat. *Journal of Neuroscience*, 17(1):190–203, 1997.
- [20] S. Spiga, G. Talani, G. Mulas, V. Licheri, G. R. Fois, G. Muggironi, N. Masala, C. Cannizzaro, G. Biggio, E. Sanna, et al. Hampered long-term depression and thin spine loss in the nucleus accumbens of ethanol-dependent rats. *Proceedings of the National Academy of Sciences*, 111(35):E3745–E3754, 2014.
- [21] J. A. Suykens and J. Vandewalle. Least squares support vector machine classifiers. *Neural processing letters*, 9(3):293–300, 1999.
- [22] S. A. Swanger, X. Yao, C. Gross, and G. J. Bassell. Automated 4d analysis of dendritic spine morphology: applications to stimulus-induced spine remodeling and pharmacological rescue in a disease model. *Molecular brain*, 4(1):38, 2011.
- [23] C. Tackenberg, A. Ghori, and R. Brandt. Thin, stubby or mushroom: spine pathology in alzheimer's disease. *Current Alzheimer research*, 6(3):261–268, 2009.
- [24] O. v. B. und Halbach. Structure and function of dendritic spines within the hippocampus. *Annals of Anatomy-Anatomischer Anzeiger*, 191(6):518–531, 2009.
- [25] Y. Zhang, X. Zhou, R. M. Witt, B. L. Sabatini, D. Adjeroh, and S. T. Wong. Dendritic spine detection using curvilinear structure detector and lda classifier. *Neuroimage*, 36(2):346–360, 2007.